DOI 10.1007/s11595-017-1683-x

Long-term Behavior of Fiber Reinforced Concrete Exposed to Sulfate Solution Cycling in Drying-immersion

GENG Yongjuan[1], JIN Zuquan[1*], HOU Baorong[2], ZHAO Tiejun[1], GAO Song[1]

(1.School of Civil Engineering, Qingdao Technological University, Qingdao 266033, China; 2 Institute of Oceanology, The Chinese Academy of Science, Qingdao 266071, China)

Abstract: The damage process and corrosion ion distribution in concrete, which was exposed to 60 and 170 drying-immersion cycles of sulfate solution, were systematically investigated. The effects of plain concrete, plain concrete mixed with 4 and 8 kg/m^3 modified PP fiber and high-performance concrete (HPC) mixed with 0.8 kg/m^3 fine PP fiber on the damage process were also studied. The experimental results showed that thenardite-induced surface scaling, as well as gypsum- and ettringite-induced cracks, were the main degradation forms of concrete under attack of sulfate solution and drying–immersion cycles. The relative dynamic modulus of elasticity of concrete initially increased, then reached stability and finally decreased to failure. The sulfate diffusion coefficients of plain and HPC were 10^{-12} and 10^{-13} m^2/s, respectively. The concentration of sodium ion increased with depth, then maintained stability and finally decreased rapidly with concrete depth. The content of calcium ion on the concrete surface was 110%-150% of that in the interior of specimens. Although fiber worsened the surface scaling of concrete, better resistance capacity of sulfate ion penetration into concrete was observed in plain concrete with 4 kg/m^3 modified PP fiber and HPC.

Key words: fiber reinforced concrete; sulfate ion; damage; diffusion coefficient; drying-immersion cycles

1 Introduction

Degradation of structural concrete components in sulfate-bearing environments has been of concern to concrete technologists since the early 19th century[1-3]. Given construction development in saline soils and salt lake areas, deterioration of reinforced concrete structures caused by sulfate attack is widely reported by researchers in China[4,5]. Important concrete structures are designed to serve for 50 to 100 years with minimal maintenance. Sulfates present in soils, groundwater and seawater pose a major threat to the durability of concrete structure exposed to such environments. Sulfate attack on concrete may lead to cracking, spalling, enlarged permeability and strength loss. Therefore, to achieve long performance, concrete in contact with sulfate-containing soil or water should be designed to resist sulfate attack.

(Received: Nov. 1, 2016; Accepted: Dec. 27, 2016)

GENG Yongjuan(耿永娟): Ph D; E-mail: gengyongjuan@126.com

* Corresponding author:JIN Zuquan (金祖权): Ph D; Prof.; E-mail: jinzuquan@126.com

Funded by the National Natural Science Foundation of China (Nos. 51378269 and 5142010501), the Chinese National Basic Research Program of China(No. 2015CB655100) and the 111 Program

Given the increased acceptability of life cycle costing of concrete structures and development of service life prediction models, determining damage process and degradation mechanism of concrete in sulfate environment is important. Corrosion expansion, which mainly involves the reaction of Na_2SO_4 with $Ca(OH)_2$ to form gypsum and the reaction of the formed gypsum with calcium aluminate hydrates to form ettringite, results in deterioration of concrete exposed to sulfate solution. Deterioration of physical properties of plain concrete in sulfate environment is also reported by many researchers[6-10]. Long-term behaviour and damage mechanism of concrete under attack of sulfate solution and drying-immersion cycles are important to determine. Sulfate ion distribution in concrete and its diffusion coefficient are promoted to predict service life of concrete. Calcium and sodium ion distribution in concrete may determine the deterioration degree of concrete and its damage mechanism. Therefore, this study aimed to determine the long-term behaviour and corrosion ion distribution in concrete exposed to drying-immersion cycles of sulfate solution.

Ordinary concrete is commonly used in tunnel lining and bridge pile cap structures in northwest China[11]. Experimental results of immersing ordinary concrete in Na_2SO_4 solution for more than 40 years

and half-burying concrete in sulfate soil for 5 years showed that fly ash and low C_3A improve the sulfate resistance capacity of concrete[2,12]. The highest land temperature in northwest China is more than 60 ℃, and rain-induced drying-wetting cycles are frequent in summer. Therefore, the damage process of ordinary concrete exposed to drying-immersion cycles of sulfate solution would be revealed. Given increased emphasis on concrete structure durability in China, high-performance concrete (HPC) is commonly used in subsea tunnels, cross-sea bridges and high-speed railways. PP fiber-reinforced concrete is often employed in areas with low RH and high temperature because PP fiber could improve the resistance capacity to shrinkage crack and high-temperature spalling of concrete[13,14]. To obtain reliable information about the influence of PP fiber on sulfate-induced damage of concrete, this paper discusses the deterioration of fiber-reinforced concrete, plain concrete and HPC in sulfate environment.

2 Experimental

2.1 Materials

Chinese standard 52.5 R(II) portland cement (similar to ASTM type I ordinary Portland cement), with 52.5 MPa compressive strength at 28 days, was used to prepare HPC. PO 42.5 ordinary Portland cement, with 51.4 MPa compressive strength at 28 days, was employed for plain concrete. The PO 42.5 cement is composed of 85% clinker, 7% limestone, 8% steel slag and 4.5% gypsum. In addition, class F fly ash and GGBS with specific surface area of 380 kg/m^3 were used as supplementary cementitious materials of the total binder. Table 1 lists the chemical composition of R(II) Portland cement, PO 42.5 ordinary Portland cement, fly ash and GGBS.

Modified PP fiber was used to prepare ordinary fiber-reinforced concrete with length and diameter of 50 and 1 mm, respectively. This concrete had a tensile strength of 410 MPa and an elasticity modulus of 4.2 GPa. Fine PP fiber with length and diameter of 10 mm and 25 μm, respectively, was employed to prepare HPC. This fiber had a tensile strength of more than 350 MPa and an elasticity modulus of 3.5 GPa. Natural river sand with a fineness modulus of 2.7-2.8 and crushed limestone with a maximum size of 20 mm were used as aggregates. The dosage of superplasticizer was adjusted to the range of 180 to 200 mm to maintain the slump of fresh concrete. The mixture proportions and corresponding compressive strengths of concrete are given in Table 2.

Table 1 Chemical composition of binders

Constituent/wt%	52.5 R(II)	PO 42.5	Fly ash	GGBS
SiO_2	21.07	22.92	52.67	33.32
Al_2O_3	3.79	7.35	33.41	13.59
Fe_2O_3	3.19	3.09	4.33	1.36
CaO	61.85	56.46	4.87	41.63
MgO	3.05	4.07	0.77	5.72
K_2O	0.61	0.49	1.04	0.46
Na_2O	0.26	0.99	0.39	0.55
TiO_2	0.24	0.35	1.46	0.6
SO_3	2.26	1.52	0.69	2.72
P_2O_5	0.08	0.05	0.34	0.04
Cl	0.039	0.05	0.018	0.007

2.2 Methods

Concrete specimens with 100 mm× 100 mm× 100 mm size were prepared to monitor the development of compressive strength and corrosion ion distribution in sulfate-bearing environment. Specimens with 100 mm× 100 mm× 400 mm size were used to monitor the ultrasonic velocity evolution in sulfate-bearing environment. All specimens were cast at room temperature in module for the first 24 h. After demolding, all specimens were cured at 20 ± 3 ℃ and 95% of relative humidity for 60 days.

The damage process of concrete under attack of erosion solution of 5% Na_2SO_4 and drying-immersion cycles was investigated. The maximum ground temperature in northwest China can reach more than 60 ℃ in summer, and temperature higher than 70 ℃ could accelerate the decomposition of ettringite. The

Table 2 Mix proportion and compressive strength of concrete

No.	kg/m^3							Compressive strength/MPa		
	Cement	Fly ash	GGBS	Sand	Aggregate	Water	Fiber	3 d	28 d	60 d
OPC	197	132	0	682	1267	170	0	16.3	28.1	36.8
FPC1	197	132	0	682	1267	170	4	16.4	28.6	32.6
FPC2	197	132	0	682	1267	170	8	14.6	27.5	32.6
HPC	250	75	145	730	1095	155	0.8	33.7	65.2	75.0

method of drying-wetting cycles proposed by Atkinson and Long was used as reference[15,16]. The drying-immersion cycles were applied in this research as follows. Concrete specimens were dried at 65 ℃ for 9 h, cooled to room temperature for 1 h and submerged in 33.8 g/L SO_4^{2-} solution (5% by mass of Na_2SO_4) at room temperature for 14 h. To determine the content of corrosion ions at different depth intervals from the concrete surface to the inner section, the specimens were allowed to dry after 60 and 170 cycles. The dried concrete specimen surface was cleaned with a steel wire brush to remove completely the salt crystals caused by corrosion. Subsequently, each specimen powder was collected from the exposed sulfate solution surface to the inner region of the specimens at regular intervals of 3-4 mm by grinding. The powder removed from specimens was dried at 50 ℃ for 10 h and passed through a 0.08 mm sieve, and the obtained powder samples were stored in airtight plastic bags. XRF was conducted to analyse sulfate and other ion contents of the powder samples.

The ultrasonic velocity of concrete was monitored every 10 cycles in sulfate environment. Based on the value of ultrasonic velocity, the dynamic modulus of elasticity (DME) could be determined using Eq.(1). The relative dynamic modulus of elasticity (RDME), which is determined by Eq.(2), is the ratio of DME value to the initial DME value after a certain exposure period. According to the test procedure of Jin[17], a specimen was considered failure if the RDME dropped to 60% or less. Three specimens were measured for each concrete mix:

$$E_{\mathrm{d}} = \frac{(1+\upsilon)(1-2\upsilon)\rho V^2}{1-\upsilon} \tag{1}$$

$$RDME = \frac{E_{\mathrm{d}t}}{E_{\mathrm{d}0}} = \frac{V_t^2}{V_0^2} = \left(\frac{T_0}{T_t}\right)^2 \tag{2}$$

where, E_{d} is the DME, V is the ultrasonic velocity (m/s), T_0 and T_t are the ultrasonic time of concrete specimens at 60 days of curing and exposure period of 't' (s), respectively, ρ is the density of specimen (kg/m^3) and ν is Poisson's ratio.

Corrosion production and pore structure of concrete specimens in sulfate-bearing environment were also tested by SEM and MIP.

3 Results and discussion

3.1 Deterioration of concrete

RDME of plain concrete, fiber-reinforced concrete and HPC stored in 5% $NaSO_4$ with drying-immersion cycles was recorded (Fig.1). The RDME of concrete in 5% $NaSO_4$ exhibited three distinct stages. In Stage I, which is from the initial corrosion to about 40 cycles, the RDME increased linearly with exposure period; thus, this stage is called 'linearly increased period.' In Stage II, the RDME was stably maintained, and this stage is denoted as 'steady period.' In Stage III, the RDME decreased with exposure cycles, and this stage is denoted as 'declining period.' The RDME value of FRC1 specimen was 1.137, which was 1.24 and 1.2 times of those of FRC2 and OPC when concrete specimens were under 170 drying–immersion cycles in sulfate solution. Thus, plain concrete with 4 kg/m^3 modified PP fiber could improve its resistance capacity to sulfate-induced damage. However, the addition of more fiber can be easily damaged by sulfate solution. In comparison, HPC exhibited good resistance capacity to sulfate-induced damage. When HPC was exposed to sulfate environment for 210 cycles, only Stages I and II occurred because of the short corrosion period.

Experimental results from Yuan[18] showed that compressive strength of concrete specimens subjected to 250 cycles of cyclic 10% Na_2SO_4 decreases by about 10% to 50% with increasing fly ash addition of 10% to 20%. Long[16] reported that the relative flexural strength ratio of ordinary concrete and concrete with 35% fly ash under 90 drying-immersion cycles is larger than 0.75 and 0.9. Compared with the abovementioned experimental results, less concrete damage was observed from the same cycles in the present experiment. The finding was attributed to

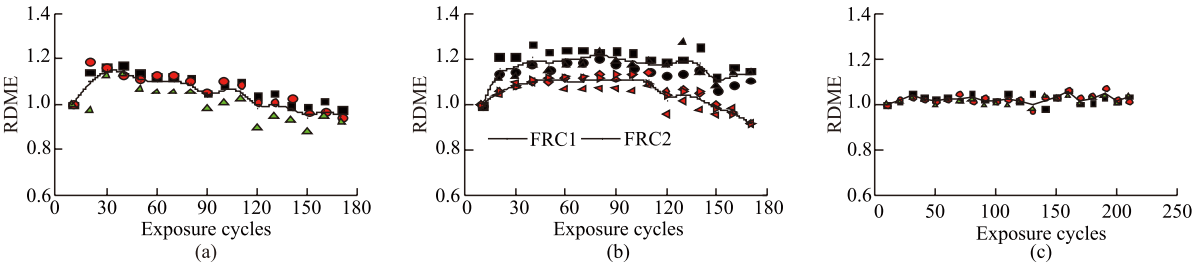

Fig.1 RDME of concrete exposed to 5% Na_2SO_4 solution and drying-immersion cycles: (a) OPC, (b) fiber-reinforced concrete and (c) HPC

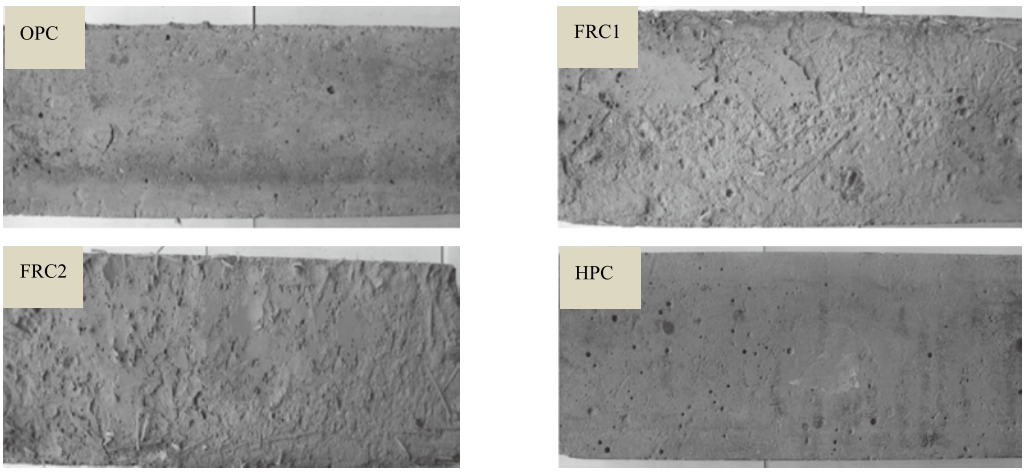

Fig.2 Surface deterioration of concrete in sulfate environment

higher temperature (drying at 80 ℃) and Na_2SO_4 concentration in solution (10% Na_2SO_4 in Yuan and 35% Na_2SO_4 in Long), which accelerated the concrete damage. Moreover, the pozzolanic reactivity of fly ash in concrete is expected to improve when concrete is cured in standard condition for 60 days and dried at 60 ℃, which increases the sulfate resistance capacity of concrete.

Irassar[12] reported that the compressive strength increases by 144% when concrete with 40% fly ash is half-buried in soil that contains approximately 1% Na_2SO_4 for 5 years. Experimental results of Zhang[19] showed that the compressive strength of concrete with 20% fly ash increases from 32.8 MPa to 50 MPa when concrete specimens are stored in 5% Na_2SO_4 for 300 days. Previous experimental results indicated that the RDME of OPC is higher than 1.07 when OPC with *w/c* of 0.44 is stored in 5% Na_2SO_4 for 830 days[17]. Compared with natural immersion, drying-immersion cycles accelerated the evolving rate of RDME and concrete damage attacked by sulfate solution. This result is mainly attributed to increased chemical reaction rate induced by high temperature and accelerated absorption of sulfate ions in concrete as a result of drying-wetting cycles.

The surface appearances of ordinary concrete specimens exposed to sulfate environment for 170 cycles and that of HPC under 210 drying-immersion cycles in sulfate solution are shown in Fig.2, which illustrates that surface scaling is the common degradation form of concrete under the attack of sulfate solution and drying–immersion cycles. The deterioration of FRC1 specimen was less than that of OPC and FRC2 specimen. The HPC possesses integrated appearance and slight damage even after exposure to sulfate environment for 210 cycles.

3.2 Sulfate ion distribution in concrete

Fig.3 shows the concentration profiles of sulfate ions at different depth intervals of concrete in sulfate environment for 60 and 170 cycles. The concentration of sulfate ions clearly decreased from the surface to the interior of concrete and reached a steady value at 6 to 15 mm depth, and the amount of sulfate ions in concrete increased with corrosion period. The profile data could be fitted by the solution of Fick's second law of unsteady state diffusion in 1D:

$$C(x,t) = C_0\left[1-\mathrm{erf}\left(\frac{x}{2\sqrt{D_{\mathrm{eff}}t}}\right)\right] \tag{3}$$

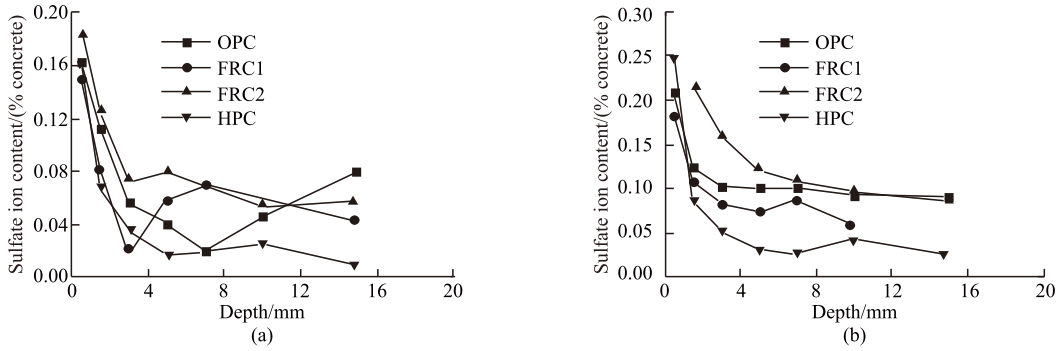

Fig.3 Sulfate ion distribution in concrete exposed to sulfate environment for 60 (a) and 170 cycles (b)

where $C(x,t)$ is the sulfate concentration for any position and time, C_0 is the sulfate concentration on the concrete surface, x is the distance from the surface, t is time, erf is the statistical error function and D_{eff} is the effective sulfate diffusion coefficient.

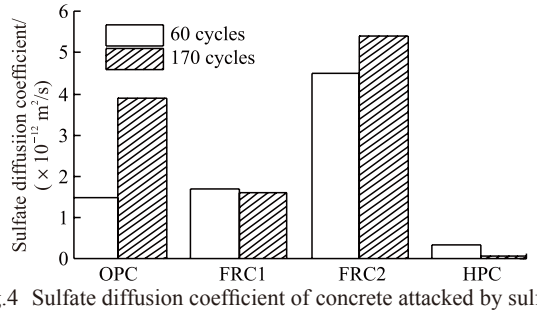

Fig.4 Sulfate diffusion coefficient of concrete attacked by sulfate solution and drying-immersion cycles

The sulfate diffusion coefficient of concrete was calculated based on Eq.(3) and plotted in Fig.4. The effective sulfate diffusion coefficient increased with corrosion time besides FRC1 and HPC specimens. Considering that the value of D_{eff} was incorporated in all sulfate transport mechanism and influenced by sulfate reaction, the sulfate resistance capacity of FRC1 was better than those of OPC and FRC2. Therefore, 4 kg/m^3 modified PP fiber could improve the resistance capacity of sulfate ion penetration into ordinary concrete. Moreover, the sulfate diffusion coefficients of HPC were 3.5×10^{-13} and 0.8×10^{-13} m^2/s for 60 and 170 cycles, respectively. Compared with ordinary concrete, the sulfate diffusion coefficient of HPC decreased by more than 10 times, which indicates that HPC has better resistance capacity to sulfate erosion than ordinary concrete.

3.3 Sodium and calcium ion distribution in concrete

Concrete stored in sulfate solution and subjected to drying-immersion cycles, as well as the concentration of sodium and calcium ions in concrete at different depth intervals, were tested (Fig.5). The sodium ion content increased from the surface to the interior, then stably maintained and finally decreased rapidly with concrete depth. The calcium ion concentration decreased with concrete depth, and the calcium ion content on the concrete surface was about 110%-150% of that in the interior. In addition, the concentration of sodium ion in concrete increased with exposure period. This result indicates that thenardite is also a main corrosion product besides ettringite and gypsum, and thenardite increased with exposure period when concrete was subjected to drying-immersion cycles of sulfate solution.

3.4 Microstructure

Ca, Si, S, and Al elements along the interface zone between cement paste and aggregate are shown in Fig.6. The silicon-rich area with white color is an aggregate. A high Ca concentration was found in paste cement. In the interface zone between paste cement and aggregate, higher levels of S and Al elements were detected. Thus, the corrosion product of ettringite was mainly generated in the interface zone.

Fig.7 shows that ettringite crystals appeared

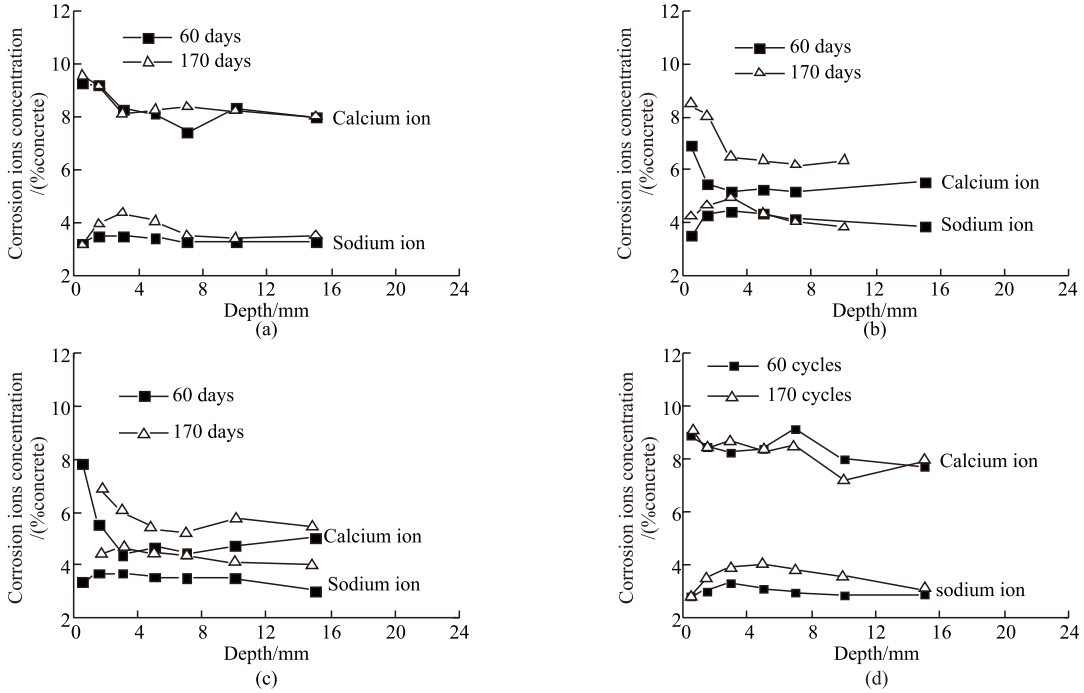

Fig.5 Calcium and sodium ion distributions in concrete: (a) OPC, (b) FRC1, (c) FRC2 and (d) HPC

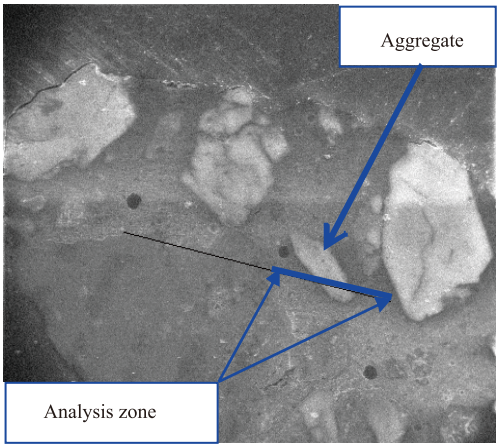

(a) Scanning area

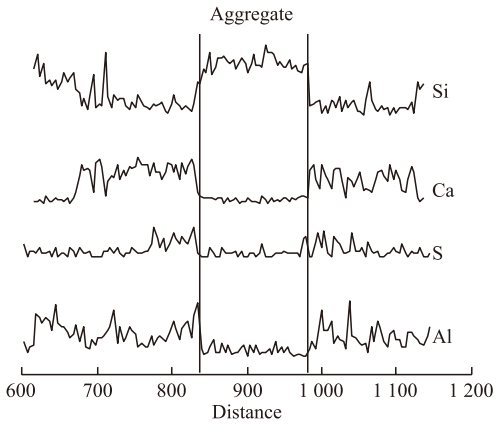

(b) Element profiles

Fig.6 Elements distributed along the interface zone

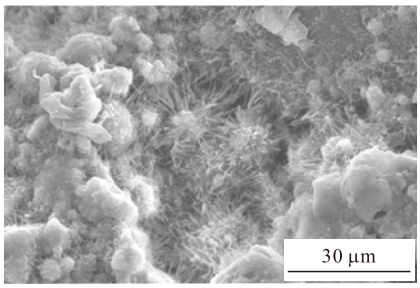

Fig.7 Ettringite generated in concrete void

in pores and voids at a distance of 760 μm from the surface, when concrete is exposed to sulfate solution and drying-immersion cycles. Based on EDS spectra and the report of Carlos[20], abundant granular thenardite formed on the specimen surface, which induced concrete spalling (Fig.8).

HPC and OPC concrete specimens exposed to 60 and 170 drying-immersion cycles of sulfate solution, as well as the pore structures of concrete at a distance of 5 mm from the surface to the interior, are shown in Figs.9 and 10.

Concrete pores with greater than 0.1 and 100 nm sizes are defined as microcrack and capillary pores, respectively. When HPC specimens were exposed to sulfate solution and 60 drying-immersion cycles, the contents of capillary pore and microcrack were 46.44% and 14.37%, respectively. For an exposed period of 170 cycles, the capillary pore and microcrack of HPC decreased by 12.7% and 62.2%, respectively. The pore structure change of HPC indicates that ettringite, gypsum and thenardite corrosion crystals compacted the pore structure and microcrack in 170 cycles. Thus,

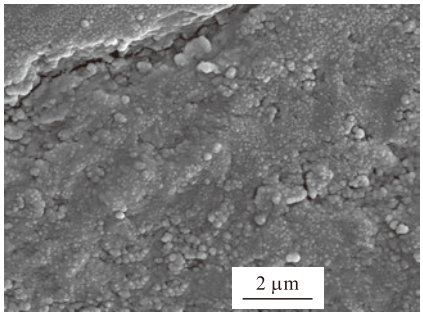

(a) Granular thenardite crystal

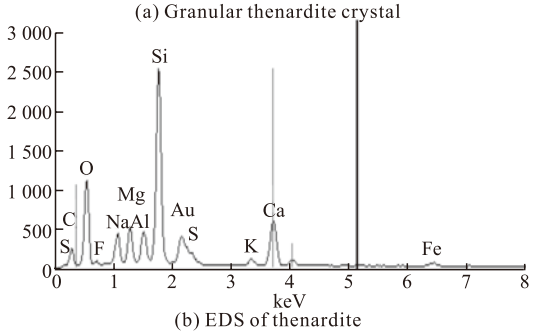

(b) EDS of thenardite

Fig.8 Appearance and EDS of thenardite in concrete exposed to sulfate solution and drying-immersion cycles

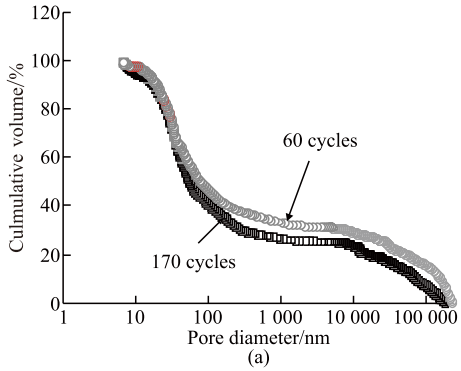

(a)

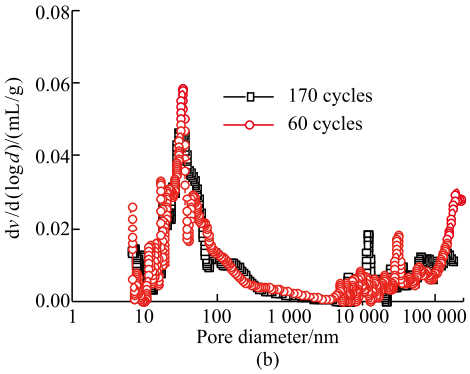

(b)

Fig.9 Pore structures of HPC under attack of sulfate for 60 and 170 cycles: (a) cumulative and (b) differential pore volumes

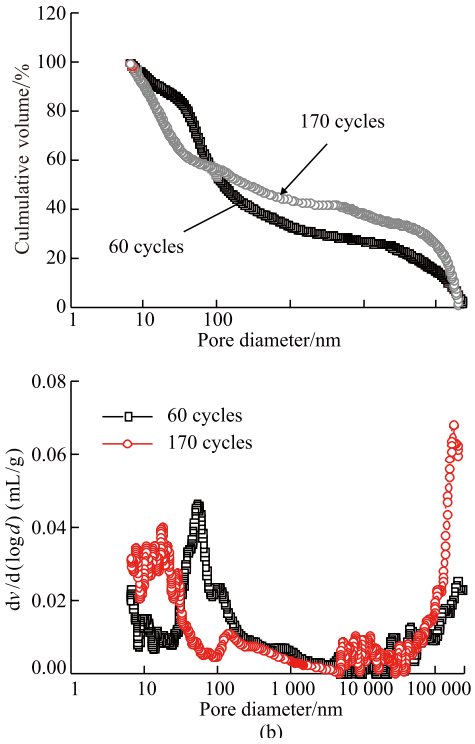

Fig.10 Pore structure of OPC under attack of sulfate for 60 and 170 cycles: (a) cumulative and (b) differential pore volumes

sulfate diffusion coefficient of HPC at 170 cycles was less than that at 60 cycles. Experimental results show that the contents of capillary pore and microcrack increased by 6% and 71.3% when OPC specimens were exposed to 60 to 170 drying-immersion cycles of sulfate solution. This finding indicates that expansion corrosion crystals initially compacted the microstructure of concrete and subsequently resulted in the appearance of cracking with further development of exposure period. The coarse pore structure and increased microcracks led to increasing sulfate diffusion coefficient from 1.5×10^{-12} to 3.9×10^{-12} m^2/s when OPC was exposed to sulfate solution and 60 to 170 drying-immersion cycles.

4 Conclusions

Ettringite, gypsum and thenardite were the main corrosion products of concrete exposed to drying-immersion cycles in sulfate solution. These expansion corrosion crystals initially compacted the pores and microcracks of concrete, and the coarse pore structure then resulted in the occurrence of cracking and surface scaling. Therefore, the RDME of concrete increased linearly with exposure period first, then stably maintained and finally decreased with exposure cycles.

Sulfate ion penetration into concrete could be fitted by Fick's second law. The calcium ion content on the concrete surface was about 110%-150% of that in the interior. The sodium ions increased with depth, then stably maintained and finally decreased rapidly with depth of concrete.

Plain concrete with 4 kg/m^3 modified PP fiber could be used to improve the sulfate resistance capacity of ordinary concrete. Low *w/b* and high content of mineral admixtures that contained fly ash and GGBS increased the sulfate erosion resistance capacity of HPC and reduced its sulfate diffusion coefficient to 10% of that of ordinary concrete.

References

[1] Rasheeduzzafar. Influence of Cement Composition on Concrete Durability[J]. *J. ACI Material*, 1992, 89(6): 574-586
[2] Monteiro PJM, Kurtis KE. Time to Failure for Concrete Exposed to Severe Sulfate Attack [J]. *Cement and Concrete Research*, 2003, 33(7): 987-993
[3] Zuo XB, Sun W, Li H, *et al.* Modeling of Diffusion-reaction Behavior of Sulfate Ion in Concrete under Sulfate Environments [J]. *Computers and Concrete*, 2012,10(1): 79-93
[4] Qiao HX, He ZM, Zhu YP, *et al*. Durability Study of High Performance Concrete in Salt Region[J]. *China Railway science*, 2007, 27(4): 32-37
[5] Ma BG, Gao XG, Byars EA, *et al.* Thaumasite Formation in a Tunnel of Bapanxia Dam in Western China[J]. *Cement and Concrete Research*, 2006, 36(4): 716-722
[6] Nehdi ML, Hayek M. Behavior of Blended Cement Mortars Exposed to Sulfate Solutions Cycling in Relative Humidity[J]. *Cement and Concrete Research*, 2005, 35 (4): 731-742
[7] Zhang MH, Jiang MQ, Chen JK. Variation of Flexural Strength of Cement Mortar Attacked by Sulfate Ions[J]. *Engineering Fracture Mechanics*, 2005, 75 (17): 4 948-4 957
[8] Jin ZQ, Sun W, Jiang JY, *et al*. Damage of Concrete Attacked by Sulfate and Sustained Loading[J]. *Journal of Southeast University (English edition)*, 2008, 24(1): 69-73
[9] Bassuoni MT, Nehdi ML. Durability of Self-consolidating Concrete to Sulfate Attack under Combined Cyclic Environments and Flexural Loading[J]. *Cement and Concrete Research*, 2009, 39(3): 206-226
[10] Rozière E, Loukili A, Hachem RE, *et al.* Durability of Concrete Exposed to Leaching and External Sulphate Attacks[J]. *Cement and Concrete Research*, 2009, 39 (12): 1 188-1 198
[11] Xie YJ, Zhong XH, Zhu CH, *et al.* Durability of HPC for Bridge and Tunnel Structure on Qinghai-Tibet Railway[J]. *China Railway Science*, 2003, 24(1): 108-112
[12] Irassar EF , Maio AD, Batie OR. Sulfate Attack on Concrete with Mineral Admixtures[J]. *Cement and Concrete Research*, 1996, 26(1): 113-123
[13] Vahid A, Togay O. Mechanical and Durability Properties of High-strength Concrete Containing Steel and Polypropylene Fibers[J]. *Construction and Building Materials*, 2015, 94(30): 73-82
[14] Saeid K, Hazizan MA, Morteza J, *et al.* The Effects of Polypropylene Fibers on the Properties of Reinforced Concrete Structures[J]. *Construction and Building Materials*, 2012, 27(1): 73-77
[15] Atkinson A, Hearne JA. Mechanistic Model for the Durability of Concrete Barriers Exposed to Sulfate-bearing Groundwater[C]. In: *Materials Research Society Symposium Proceedings*, 1990 (176): 149-156
[16] Long GC, Xie YJ, Tang XG. Evaluating Deterioration of Concrete by Sulfate Attack[J]. *Journal of Wuhan University of Technology-Mater. Sci. Ed.*, 2007, 22(3): 572-576
[17] Jin ZQ, Sun W, Zhang YS, *et al*. Interaction Between Sulfate and Chloride Solution Attack of Concrete With and Without Fly Ash[J]. *Cement and Concrete Research*, 2007, 37(8): 1 223-1 232
[18] Yuan XL, Li BX, Cui G, *et al.* Effect of Fly Ash and Early Strength Agent on Durability of Concrete Exposed to the Cyclic Sulfate Environment[J]. *Journal of Wuhan University of Technology-Mater. Sci. Ed.*, 2010, 25(6): 1 065-1 069
[19] Zhang JS, Zhang YH, Feng LP. Corrosion Resistance Coefficient for Concrete Compressive Strength under Sulfate Environment[J]. *Journal of Building Materials*, 2014, 17(3): 369-377
[20] Carlos RN, Eric D, Eduardo S. How Does Sodium Sulfate Crystallize Implications for the Decay and Testing of Building Materials[J]. *Cement and Concrete Research*, 2000, 30(10): 1 527-1 534